Chapter 8
Future Directions in Advanced Mycological Microscopy

Kirk J. Czymmek and Tanya E. S. Dahms

8.1 Introduction

Recently, a truly remarkable series of innovative technical advances in cell biology tools have opened the door to new discoveries and ultimately a much deeper understanding of many biological phenomena. Indeed there are so many innovations, with often subtle variations, that it can be a significant challenge to identify which tool/approach is the most appropriate to address a scientific question. While the pace of progress is quite extraordinary, we welcome these advances that are quickly overcoming technological barriers/limitations of even just a few years ago. While these developments are exciting, this virtual renaissance for cell biologists and microscopists requires us to keep an ever-vigilant eye for the quick adoption of new strategies as appropriate. Fungal cell biologists are well positioned to leverage these advances due to the inherent microscopic dimensions of many fungal structures, suitable model organisms and their fundamental importance in our day-to-day life in relation to food, medicine, and disease.

In this chapter, our focus on future directions turned to select imaging topics that we believe have great potential to transform how we understand mycological research, including fungal interactions with the environment and other organisms. We not only place special emphasis on correlative microscopy (light, electron, and scanning probe), but also include the interrelated topics of advanced three-

K. J. Czymmek (✉)
North American Applications and Labs, Carl Zeiss Microscopy, LLC, One Zeiss Drive, Thornwood, NY 10594, USA
e-mail: Kirk.Czymmek@zeiss.com

T. E. S. Dahms (✉)
Department of Chemistry and Biochemistry, University of Regina, Regina, Saskatchewan S4P 1N7, Canada
e-mail: tanya.dahms@uregina.ca

T. E. S. Dahms and K. J. Czymmek (eds.), *Advanced Microscopy in Mycology,* Fungal Biology, DOI 10.1007/978-3-319-22437-4_8

dimensional (3D) electron microscopy and fluorescent biosensors. We consider all of these approaches naturally intertwined as key imaging building blocks that, when used together, significantly amplify the benefits and power of the individual tools.

8.2 Advances in the Application of Biosensors

As demonstrated throughout this book, fungal cell biology has benefited from an array of contrasting and complementary strategies that allow visualization of gross fungal structures, individual cells, subcellular compartments, and macromolecules. A great emphasis has been placed on understanding the polarized hyphal tip, and rightly so as it is the dominant form of fungal growth. Indeed, various fluorescent probes including small molecules (Kankanala et al. 2007; Hickey et al. 2004) and genetically encoded protein fusions (Czymmek et al. 2002, 2004, 2005) have been a boon to our understanding of tip growth. However, in fungi, fully realizing the significant progress demonstrated in plant and mammalian cell systems has been challenging, especially with genetically encoded biosensors for imaging ions, molecular interactions, and cell signaling dynamics. The vast majority of biosensors exploit Förster resonance energy transfer (FRET)-based folding/unfolding of a target protein that is a chimera with a pair of spectrally overlapping fluorescent proteins (FPs) to reveal dynamic and measurable responses. However, intensity and spectral changes (Miesenböck et al. 1998) and single fluorophore complementation strategies (Akerboom et al. 2012) can also be detected with single FP sensors. While no fundamental barriers prevent the application of genetically encoded biosensors in fungi, with numerous examples of standard FP fusions in the fungal kingdom (Chaps. 1–3; Czymmek et al. 2004), there are surprisingly few published examples. As such, we suggest that there are significant opportunities for new discoveries using biosensors to probe the inner workings of fungal cells. One conspicuous example is the ubiquitous calcium ion which as a universal secondary messenger in biological systems has been one of the best studied ions. However, visualizing calcium ion dynamics using organic fluorescent dyes in fungi has met with limited success, driving the use of FP-based calcium ion sensors, already widely used in animal and plant biology (Newman et al. 2011; Okumoto et al. 2012). Toward this end, the bioluminescent aequorin gene from the jellyfish *Aequoria victoria* was successfully expressed in fungi to determine cytosolic calcium concentration ($[Ca^{2+}]_c$) (Nelson et al. 2004). The study required significant effort to optimize codon usage but was rewarded with successful time-based calcium signaling, monitoring in populations of cells for the first time. Subsequently, successful expression and imaging of Cameleon YC3.60 (Nagai et al. 2004), the calmodulin-based $[Ca^{2+}]_c$ FRET sensor, in three economically important plant pathogenic fungi, *Magnaporthe oryzae, Fusarium oxysporum,* and *Fusarium graminearum* (Kim et al. 2012), was demonstrated. In this work, age/development dependent and pulsatile subcellular calcium dynamics and transient tip high $[Ca^{2+}]_c$ gradients were observed in various stages of vegetative growth and disease.

Genetic encoding can help circumvent the recalcitrant properties of the fungal cell and its tendency to sequester or otherwise compartmentalize/degrade exogenously introduced fluorescent probes, rendering them ineffective (Hickey et al. 2004). For those genetically tractable species, codon optimization and construct modification will likely be required along with species-dependent strategies. The array of biosensors already available and used in mammalian and plant cells can serve as a starting point for real-time monitoring of cellular activity. Those monitoring pH (Miesenböck et al. 1998), promotor activity (Terskikh et al. 2000), protein turnover (Subach et al. 2009), translocation (Varnai and Balla 2007), protease (Xu et al. 1998; Luo et al. 2001) calcium ions (Miyawaki et al. 1997; Kim et al. 2012; Akerboom et al. 2012), adenosine triphosphate (ATP; Imamura et al. 2009), cyclic adenosine monophosphate (cAMP; Zaccolo et al. 2000), cyclic guanosine monophosphate (cGMP; Honda et al. 2001; Sato et al. 2000), G-protein (Pertz et al. 2006) and kinase activation (Schleifenbaum et al. 2004), reactive oxygen species (ROS; Belousov et al. 2006), and membrane potential (Tsutsui et al. 2008) will allow many critical fungal processes to be explored in real time. Of course, many of these sensors can be applied in concert with other FP fusions and vital dyes that target organelles, cytoskeletal, and other proteins. We hope our readers will see the merit in exploiting biosensors in their own research projects and we encourage you to explore the possibilities (Reviewed in Frommer et al. 2009; Newman et al. 2011; Okumoto et al. 2012).

8.3 Three-Dimensional Electron Microscopy

Fungal structures, such as organelles, cells, mycelial networks/tissues, and fungal host/surface interactions, are inherently 3D. A far greater understanding of the structure–function relationship in these cells and tissues is now achievable with high-resolution correlation of chemical markers and structural components in the third dimension. Transmission electron microscopy (TEM), a mainstay in high-resolution fungal cell biology, especially when combined with freeze-substitution, antibody/affinity probe gold localization, and serial section analysis (Howard and Aist 1979), has tremendously impacted our understanding of hyphal tip architecture and function. TEM tomography, which typically generates tilt series (i.e., +/− 70°) and creates 3D data sets from back projections (Harris et al. 2005; Hohmann-Marriott et al. 2006), provides unprecedented quantitative and structural perspectives of hyphal tip organization. While TEM is the gold standard for high-resolution ultrastructure, field emission scanning electron microscopy (FESEM) can now accommodate resin embedded samples that have been physically sliced into sections on a standard ultramicrotome mounted serially on tape, glass slide, or slotted grid, each substrate having unique benefits. Modern FESEMs are highly versatile and can image stained ultrathin sections with backscattered electron (BSE), secondary electron, and scanning transmission electron detectors yielding a TEM-like image. Alternatively, 3D tomograms of sliced volumes, much like TEM, can be automated

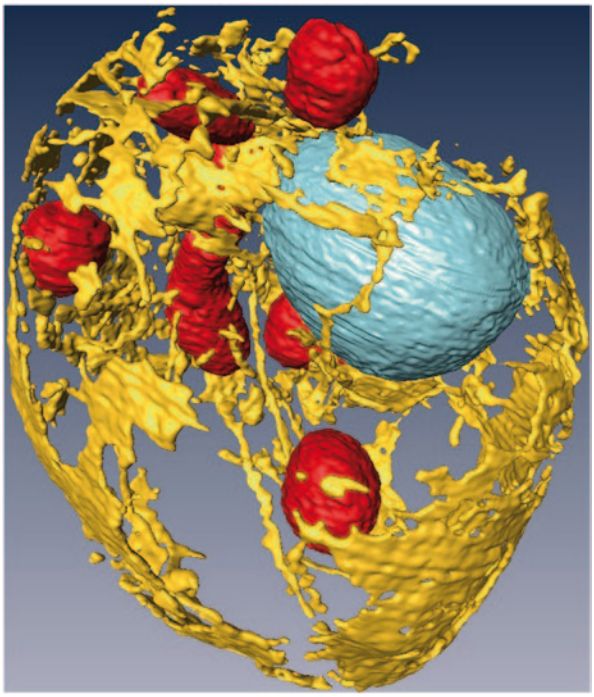

Fig. 8.1 High-resolution 3D reconstruction of a single cell of *Saccharomyces cerevisiae* acquired using focused ion beam scanning electron microscopy (*FIBSEM*; Chap. 6). The high-pressure frozen freeze-substituted, epoxy embedded yeast samples were acquired at 5 nm isotropic voxels. The *FIBSEM* approach enables extended 3D volumes of fungal structures, subcellular organelles and molecules at resolutions associated with electron microscopy. The nucleus is shown in *light blue,* mitochondria in *red,* and endoplasmic reticulum in *yellow*. Details of the protocols and findings can be found elsewhere (Wei et al. 2012). (Image provided courtesy of Jeff Caplan and Kirk Czymmek)

with serial block-face imaging (Helmstaedter et al. 2008) in which an ultramicrotome is either integrated directly into the electron microscope chamber (Denk and Horstmann 2004; Hughes et al. 2014) or a focused ion beam (FIB; Chap. 6; Wei et al. 2012) is used to mill away the specimen. FESEM approaches have a significant advantage over TEM for examining larger samples and producing extended 3D data sets of larger tissue areas (i.e., 100s of microns volumes or several millimeters section slices). These types of dimensions are particularly suitable for more complex fungal tissues and fungal–host interactions, able to resolve individual cells and even organelles. For example, the 3D reconstructions of entire high-pressure frozen yeast cells by FIB/FESEM down to ~3–5 nm are isotropically resolved (Wei et al. 2012; Fig. 8.1). These images have significantly lower physical distortions as a result of material removal as compared to classical serial thin sections, and thus the associated 3D EM reconstructions align closely with the 3D light microscopy (LM) volume image (Narayan et al. 2014). Indeed, 3D EM data also can be directly

and readily correlated with 3D LM, and X-ray micro computed tomography (Handschuh et al. 2013) and/or super-resolution images, as an extension to traditional correlative light and electron microscopy (CLEM) approaches (Caplan et al. 2011; Smith 2012; Perkel 2014).

8.4 Correlative Microscopy

Given that the power of any given method is often amplified when combined with other techniques (Smith 2012), we will focus on several advances in correlative microscopy. Combining information from two or more microscopic modes offers interpretive value that is greater than the sum of each data set alone. While fungal specific examples in the literature are relatively sparse, any of the microscopic methods discussed in this volume have the potential to be correlated and applied to modern mycology. Correlative microscopy can be generally classified into two categories: those that correlate data sets collected separately on individual microscopes, and those collected from fully integrated microscopy platforms capable of simultaneous imaging. If you have ever screened a sample on one microscope, typically with a large field-of-view and noted regions of importance prior to examination with a higher resolution microscope, then you have participated in basic correlative imaging. Indeed, the use of LM to screen samples for TEM gave rise to the now well-established term CLEM. The various microscopic modes have inspired myriad combinations of correlative microscopy as reviewed by Caplan et al. (2011). Here we describe new combinations and those we think are particularly applicable to mycology.

Multi-instrument Correlative Approaches Correlating data on the exact same region of a specimen using more than one microscope typically with the aid of masks, grids, and maps, requires highly skilled operators. As such, commercial solutions have been developed that seek to automate the tedious relocation steps (Perkel 2014; Smith 2012). Scanning electron microscopes (SEM), in particular field emission SEM (FESEM), are especially well suited to automation and have the advantage of allowing much larger serial sections to be collected on a single coverslip, glass slide, or silicon nitride wafer (Micheva and Smith 2007; Hayworth 2014). The use of silicon nitride substrates also facilitates successive TEM and tip-enhanced Raman spectroscopy (Lausch et al. 2014) that could serve as a new correlative approach for fungi.

Imaging fungal tissue structures such as fruiting bodies, plant–host interactions, or even larger scale colonies in culture could readily benefit from large-area imaging. The more automated approaches strategically place three fiducials on the substrate or sample holder for calibration on an LM. Relative coordinates are saved in the image file for rapid and precise relocation on a second microscope within minutes (i.e., FESEM). Such an approach was applied to collect structural illumination microscopy (SIM) and direct stochastical optical reconstruction microscopy (dSTORM) data using ultrathin sections of high-pressure frozen, freeze-substituted

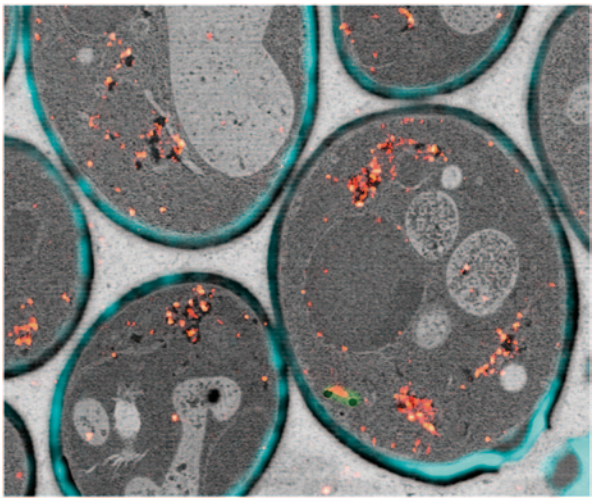

Fig. 8.2 CLEM using super-resolution with FESEM (Auriga Crossbeam, Zeiss) on thin sections of high-pressure frozen freeze-substituted *Saccharomyces cerevisiae*. Yeast cell walls *(blue)* labeled with Calcofluor white and Adenosin receptor *(red)* fused to Cerulean (hA1aR-Cerulean) and labeled with AlexaFluor®647 conjugated antibodies were imaged with structural illumination microscopy *(SIM)* and dSTORM localization microscopy, respectively, prior to additional heavy metal staining for FESEM. *BSE* images were acquired following automated recovery using Shuttle & Find software. Electron-dense cisternal compartments (Golgi equivalents) in FESEM image were directly correlated to hA1aR-Cerulean localization using dSTORM. (Image provided courtesy of Carissa Young, Jeff Caplan and Kirk Czymmek)

yeast samples embedded in HM20 resin (Fig. 8.2). Fluorophore labeled sections (AlexaFluor 647 anti-green fluorescent protein (GFP) antibody and Calcofluor counterstain) were then stained with heavy metals, moved to an FESEM, automatically relocated using correlative software and imaged using a BSE detector. Such an approach is fully amenable to widefield, confocal, and other optical microscopes. In particular, localization of single-molecule fluorescence on thin sections has some distinct advantages to traditional immunogold approaches, namely much higher labeling density and many more probes for targeting cell structure on a single section using Exchange-PAINT (Jungmann et al. 2014) or antibody stripping (Micheva and Smith 2007). Exchange-PAINT is a clever strategy that uses small, transiently binding fluorescent oligonucleotides coupled with affinity probes (biotin/antibodies) which can be multiplexed in series. Virtually an unlimited number of fluorophores can be used at each probe binding site for super-resolution single-molecule localization techniques (see Chap. 3).

Integrated Correlative Approaches Most modern microscopes have multiple optical components, for example, a typical LM will often be furnished with optics for bright-field, dark-field, phase contrast, or differential interference contrast (DIC). In this case, data correlation is straightforward since images are collected from multiple modes on a single region of the sample. Simultaneous multimode imaging

requires more than one detector port and thus the full integration of two or more microscopes with pre-calibration or post-processing to ensure that the final images are in direct correspondence. Even for fully integrated microscopes with multiple detectors, the different time scales of each microscopic mode can present a challenge for simultaneous imaging and may also require time syncing of images.

With integrated LM/TEM approaches, thin resin sections are prepared for LM image acquisition within the TEM followed by sample reorientation and TEM imaging at the same location (Agronskaia et al. 2008). An elegant extension of this approach allows frozen/hydrated samples to be maintained at cryogenic temperatures within the TEM (Faas et al. 2013). Likewise, a modified optical microscope can be accommodated within an SEM chamber (Chap. 6) using high numerical aperture (oil immersion objectives), not possible with TEM approaches (den Hoedt et al. 2014). There are three major considerations when applying integrated CLEM approaches: (1) the impact of electron–sample interactions requires that organic fluorescent probe imaging precedes EM, since the electron beam can destroy fluorescence signal; (2) modification of labeling/staining strategies may be required to avoid quenching of fluorescence signals by proximal heavy metal stains; and (3) the impact of morphological distortions from changes in cell structure during sample processing. While integrated CLEM microscopes are not widely available, we do anticipate that this will change over the coming decade and prove to be particularly useful for correlative experiments on thin resin or cryo-sections of fungal specimens. Possibilities for cryopreservation, in particular, are intriguing to maintain high-fidelity sample structure and enable snapshots of living systems using integrated instruments such as LM/SEM (Kanemaru 2009), atomic force microscopy (AFM)/SEM (Williams et al. 2002), and AFM/microtome (Effimov et al. 2007).

The full integration of atomic force and optical microscopes is now mainstream for biological studies (Fig. 8.3). This combined correlative optical and physical scanned probe strategy permits targeting of desired cells, structures, and/or phenomenon with an optical microscope for subsequent high-resolution surface imaging, mechanical, and biochemical measurements (see Chap. 7; Kaminskyj and Dahms 2008). An early integrated scanning force-light microscope used surface imaging and optical sectioning with DIC to examine how the 3D dynamic cellular organization affects surface properties (Stemmer 1995). Combining these two instruments (Nagao and Dvorak 1998) came at the expense of each experiencing additional noise: vibrations impacted AFM imaging and red light from the AFM optical lever (Chap. 7) convoluted optical images. Optical microscope mounts that coupled vibrational noise into the AF microscope were eliminated with piezo-driven active vibration isolation units (Sandercock 1987), alongside replacing the red laser component of the AFM optical lever with an infrared (IR) laser (Gamble and West 1994). For biological applications, typically the AFM and its stage are seated on an inverted optical microscope which serves several purposes: aligning the detection laser on the AFM tip (Fig. 8.3a; Chap. 7; Fig. 7.1), previewing the sample (Fig. 8.3b, i.e., choosing a peripheral hypha from a mycelium or one yeast cell), and imaging gross phenotypic or morphometric features prior to high-resolution imaging (Fig. 8.3c).

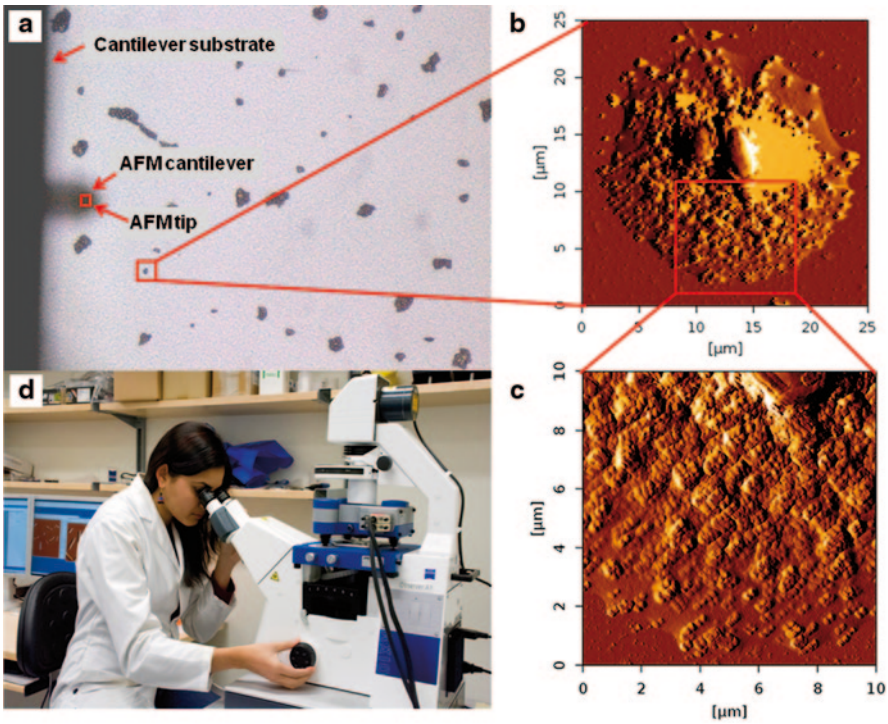

Fig. 8.3 Images of a *Candida albicans* deletion mutant exposed to 0.4 µg/ml caspofungin. **a** LM image (200×) of yeast on a glass substrate with *red arrows* indicating the out of focus AFM cantilever substrate, AFM cantilever, and AFM *tip* position. Corresponding AFM images at **b** *low* (200 × 200 pixels) and **c** *high* (500 × 500 pixels) resolution imaged in contact mode at 0.2 Hz with silicon nitride cantilevers (AppNano Hydra2R-50NG-10; nominal k ~ 0.084 N/m and radius of curvature < 10 nm) with *Z*-scale rendered in *brown (low)* to *white (high)* and fields of view as *red squares*. **d** Doctoral candidate Supriya V. Bhat examining her specimen (Bhat et al. 2015a, b) on a bright-field inverted microscope with *DIC* optics and modified condenser (Zeiss Axio Observer A1) housing an AF microscope outfitted with custom stage (JPK Nanowizard) all mounted on a piezo-driven vibration isolation platform (Herzan TS-150) and a small optical table (Halcyonics i4). Housed in the same room, on which the AFM can also be mounted, is a fluorescence microscope (Zeiss Axio observer Z1; λ_{ex} 365–580 nm) and a confocal laser scanning microscope (Ziess 780 with 458, 514, 488, 543, 594, 633 nm and pulsed two-photon Ti:Sapphire lasers) for multi-wavelength 3D imaging and FCS. (AFM images are courtesy of Spencer Zwarych and photograph by Geremy Lague)

Most commercial AFMs and optical microscopes can be integrated, with vendor choice mostly related to instrument features that satisfy user needs. A typical, relatively low-cost set-up (Fig. 8.3d) consists of an AFM outfitted with a custom stage mounted on a bright-field inverted microscope with fluorescence and/or DIC optics and modified condenser housed on a piezo-driven vibration isolation platform seated on a small optical table. The Dahms lab instrument in such a configuration (Bhat et al. 2015a, b) is capable of angstrom-scale resolution even without a sound isolation hood, despite its location on the fifth floor of their research building. Of

course, the number of additional optical components is only limited by space and budget, and AFM instruments with portable electronic control units (ECU) can be mounted on multiple microscopic platforms. For instance, the Dahms lab AF microscope (Fig. 8.3d) remains in the configuration described above for routine imaging, but can be mounted on other nearby multiuser microscopes, namely an automated fluorescence microscope and a laser scanning confocal microscope (LSCM). The LSCM is equipped with both continuous wave and pulsed two-photon (Ti:Sapphire) lasers for multiwavelength excitation during confocal imaging (3D reconstruction) and fluorescence correlation spectroscopy (FCS; reviewed in Bacia and Schwille 2003), respectively. Any fluorescence or confocal (Chaps. 1–3) microscopy method can be simultaneously recorded with any AFM parameter (Chap. 7). The Dahms group is currently developing high-content atomic force confocal assays to probe changes in microbial phenotype, morphometrics (cell size/shape), cell wall ultrastructure and integrity (AFM; Ma et al. 2005, 2006; Kaminskyj and Dahms 2008; Jun et al. 2011; Paul et al. 2011; Bhat et al. 2015a, b) concurrently with intracellular physiological stress responses tracked by confocal (Chap. 1). Sample preparation methods developed for imaging growing hyphae (Ma et al. 2005; Paul et al. 2012) and yeast (Chap. 7) by AFM enable these high-content assays of live fungi.

High-resolution Fourier transform infrared spectroscopy (FTIR) mapping has found great utility in mycology (Chap. 4), but the spatial resolution and sensitivity have been limited by the relatively long wavelengths of IR light. Synchrotron infrared nanospectroscopy (SINS) overcomes this limitation by coupling synchrotron IR radiation with an AFM (Bechtel et al. 2014), enabling AFM imaging and near-field broadband IR spectroscopy with a tip-limited spatial resolution of < 30 nm (Berweger et al. 2013). This scattering scanning near-field optical microscopy (s-SNOM) technique focuses synchrotron IR light onto the oscillating tip of a modified AFM, located within an asymmetric Michelson interferometer. Detection of the elastically scattered light at harmonics of the tip oscillation frequency discriminates the near-field signal from the far-field background (Hillenbrand 2001). Movement of the reference arm mirror enables the weakly scattered signal to be frequency resolved and amplified by the stronger reference beam (Fig. 8.4a). Fourier transformation of the resultant interferogram produces a near-field spectrum (Bechtel et al. 2014) with a probing depth < 100 nm from the outer surface of the sample. The synchrotron source provides full mid-IR coverage from 700 to 5000 cm^{-1}, limited only by the choice of beamsplitter and detector. A high-resolution AFM image not only yields surface ultrastructural data but also yields a map to precisely localize the region of interest for FTIR (Fig. 8.4b). The SINS spectrum has signal-to-noise (S/N) ~ 100-fold better than standard FTIR microscopy. However, since this approach probes only ~ 30 nm into the cell wall in a 1 μm^2 area, as opposed to the entire cell, the realized S/N improvement is far greater (Fig. 8.4c). SINS of fungal hyphae at the Advanced Light Source (ALS) at UC Berkeley is currently limited by sample preparation (air drying) and data collection times for AFM (raster scan) and FTIR spectra, which could be overcome using an inline cryo stream, high-speed AFM (HS-AFM, Sect. 5) and more sensitive IR detectors, respectively. Despite its current limitations, the SINS instrument provides spatially resolved surface ultrastructure and chemistry of fungal cell walls (Fig. 8.4).

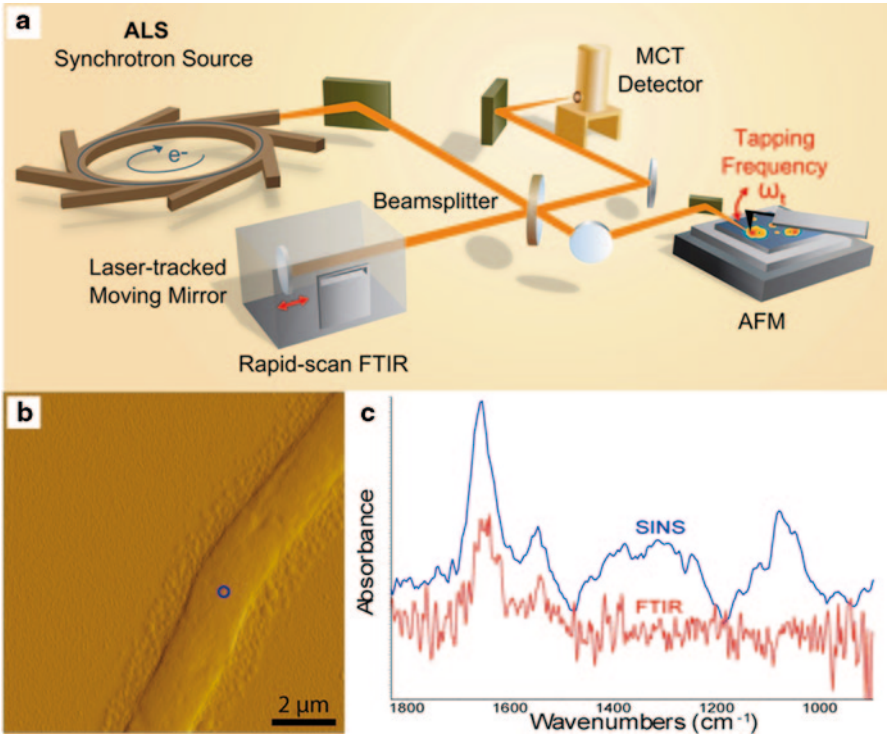

Fig. 8.4 **a** Schematic of the synchrotron infrared nano-spectroscopy *(SINS)* beam line at the 5.4.1 IR end station, at the Advanced Light Source, LBNL, Berkeley, CA, reprinted with permission from Bechtel et al. (2014). **b** AFM image of A1149 hypha approximately 15 µm behind the growing tip, acquired at the *SINS* end station. **c** *SINS* spectrum *(blue)* of the A1149 hyphal wall compared to a spectrum *(red)* of the same hypha using transmission with standard FTIR spectromicroscopy. Spectra were off set for easier visual comparison. The *SINS* spectrum shows a well-defined profile and approximately 100-fold improvement in S/N. The *SINS* spectrum in the near-field only probes the outer cell wall to approximately 30 nm depth, as evidenced from the high sugar content in the bands between 1200 and 1000 cm^{-1}, while the standard FTIR microscopy spectrum represents data from the entire cell, yielding a voxel of about 1 μm^3. The actual improvement in S/N is thus many orders of magnitude greater. (Schematic provided by Dr. Hans Bechtel, AFM image and FTIR spectra courtesy of Dr. Kathleen Gough)

Integration of super-resolution (Chap. 3) and other optical microscopes with AFM (Chap. 7) leads to intriguing possibilities. For example, combining AFM and stimulated emission depletion (STED) offers high-resolution intracellular fluorescence, topographical, and nano-mechanical imaging of cells (Chacko et al. 2013b; Harke et al. 2012) and cellular level nanomanipulation (Chacko et al. 2013a, 2014; Chap. 6). Stochastic optical reconstruction microscopy (STORM)-AFM has also been applied to study cell cytoskeleton (Chacko et al. 2013b) and surfaces (Zhao et al. 2014), and *in vitro* nucleic acid studies (Monserrate et al. 2014). Alternatively, combining AFM with synchronized confocal fluorescence lifetime microscopy (FLIM, Chap. 2), capable of tip-induced fluorescence quenching, yields

fluorescence lifetime images that can be correlated with nanometer resolution (Schulz et al. 2013), which may allow for a more detailed understanding of hyphal development, and the impact of genetic deletion of antifungal targets or exposure to antifungal agents (Chap. 7). Using multiphoton excitation (Chap. 1) for correlative second harmonic generation along with photoacoustic modes for the label-free visualization of muscle and melanocytes in zebrafish larvae *ex vivo* (Shu et al. 2014) could prove very useful for examining fungal mycelia. When AFM is part of a total internal reflection fluorescence (TIRF) system, it can probe surface receptors (Lal and Arnsdorf 2010) with the potential for mapping fungal surface molecules.

Many hybrid microscopes are exclusively optically based. The adaptation of Raman microspectroscopy (RM) to fluorescence microscopy was used for correlative chemical analysis and fluorescence imaging of proteins and lipids in blood cells (van Manen and Otto 2007). This approach would have intriguing implications if applied to the work of Chang et al. (2010) exploring label-free spatiotemporal characterization of oxidative destruction of intraphagosomal yeast *in vivo* (autofluorescence imaging and RM). Similarly, label-free imaging approaches by Li et al. (2014) exploited RM with dark-field imaging in addition to fluorescence.

A number of optical imaging techniques have also been effectively combined with microfluidics to probe biological systems (reviewed in Wu et al. 2012), for example, exploring biofilms using microfluidic total internal reflection (TIR) and TIRF microscopy (Le et al. 2009). Examining biofilms by LSCM (Chap. 1) with confocal RM shows that lipids are key in biofilm formation across diverse phyla of bacteria from the environment, can define attachment phenotypes associated with various substrata, and identify key macromolecules involved in the attachment process (Andrews et al. 2010). The heterogeneity of matrix components and the function of multiple species in complex natural biofilms within their physicochemical microenvironment (Reuben et al. 2014) can be tracked with integrated LSCM (Chap. 1) and synchrotron radiation-FTIR microspectroscopy (Chap. 4). We believe these powerful correlative tools for understanding biofilm structure and biology could be readily extended to fungal biofilm investigations.

8.5 New Imaging Technologies

The synergistic development of biosensors and imaging technologies has resulted in the very high potential for new insights in mycology. Fluorescence imaging approaches, including confocal microscopy and epifluorescence imaging in their various forms (Chaps. 1–2), will continue to be fundamental and readily available tools for fungal biology into the foreseeable future. However, super-resolution microscopy (Chap. 3; Young et al. 2012) is ideally positioned to enhance our imaging and understanding of fungal molecules and structures. While there are numerous strategies to break the diffraction limit (Chaps. 2 and 3), we would like to highlight and emphasize two that could have exceptional promise for fungal studies, 3D localization (Baddeley et al. 2011) and Airyscan (Weisshart 2014) microscopy. Furthermore, we bring attention to two additional technologies, Bessel beam planar

illumination (Planchon et al. 2011) and HS-AFM (Ando et al. 2013) which both greatly increase acquisition speed for photon- and scanning probe-based imaging, respectively.

Improvements in resolution are often accompanied by trade-offs that can limit the scope and kinetics of the biological question (i.e., requiring multiple image acquisition, significant processing time, and/or high laser powers). 3D localization microscopy is the highest resolution approach (~20 × 20 × 50 nm, *x*-*y*-*z*; Baddeley et al. 2011) with sub 10 nm resolution possible using improved probe strategies (Jungman et al. 2014). A common form of 3D localization microscopy requires that an asymmetrical point spread function (PSF) is produced by inserting an astigmatic lens or phase ramp into the light path (Baddeley et al. 2011). As a result, when single fluorescent molecules are imaged, the in-focus and defocused PSFs will have a characteristic shape relative to their position and distance from the focal plane. Since the PSF shape for each single molecule in the image is highly *z*-position sensitive, it can be modeled and a high-resolution 3D spatial map created (Baddeley et al. 2011). Typically, the rapid decline in signal, when imaging a single molecule in a diffraction-limited spot, leads to approximately 1 μm depth-of-field with 50 nm *z*-resolution for any given image. However, by taking 3D localization images at different *z*-planes, entire cells can be captured. Fixation is critical for super-resolution microscopy of fungi, as artifacts arising from movement (i.e., redistribution of cellular organelles/proteins/structures) are well known to be a particular challenge (Howard and Aist 1979). Fortunately, genetically encoded FPs for localization microscopy (Young et al. 2012) are compatible with freeze-substitution, minimizing these concerns. Indeed plunge-frozen freeze-substituted hyphal tips of *F. graminearum* expressing a calmodulin-mEos3 chimera have been imaged using 3D localization microscopy with multiple *z*-planes (Fig. 8.5). When FP fusions or genetic transformations are not possible, sample preparation using antibodies with confocal microscopy in freeze-substituted fungi (Bourett et al., 1998; Riquelme et al. 2002) could be slightly modified. Furthermore, the use of camelidae nanobodies, small (~3 nm) antigenic units derived from camels (Chavarty et al. 2014; Ries et al. 2012) would expand the applicability of 3D LM for fungi.

The addition of an Airyscan detector to an LSCM offers significant enhancement in resolution (1.7-fold over widefield) and sensitivity (Weisshart 2014). Instead of collecting a fluorescence emission signal from an LSCM at a single pinhole (see Chap. 1), it is focused on an array of 32 detectors. In confocal microscopy, decreasing the pinhole diameter improves resolution (and confocality), but at the significant cost of detection efficiency and S/N. With an Airyscan detector, while each detector element in the array is equivalent to 0.2 Airy unit (A.U.),[1] the entire array is effectively equivalent to collecting signal from a much larger 1.2 A.U. pinhole aperture

[1] Airy disk refers to the diffraction pattern of concentric circles surrounding a bright central spot created from a focused lens (Abbé 1873). The diameter of the first-order central Airy disc, objective lens dependent, is 1 A.U. The LSCM pinhole is typically set to an optimal signal-to-noise and resolution at ~1 A.U. Smaller pinholes (i.e., 0.2 A.U.) theoretically provide better resolution at the expense of signal-to-noise in a traditional LSCM setup (Chap. 1).

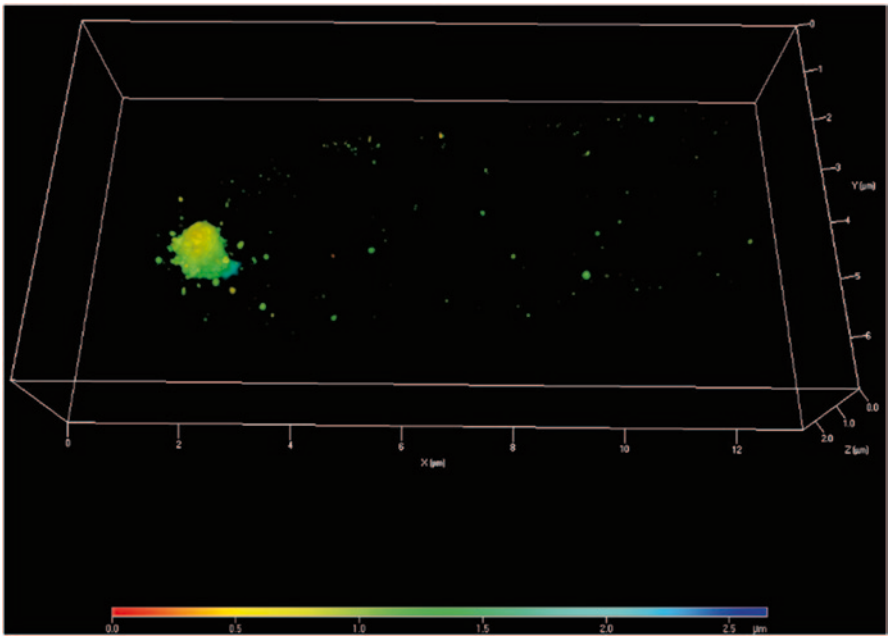

Fig. 8.5 3D photoactivated localization microscopy *(PALM)* shows super-resolution distribution of calmodulin in *Fusarium graminearum*. Expression of CaM-mEOS2 in *F. graminearum*, followed by plunge-freezing and freeze-substitution in aldehyde, revealed calmodulin localization at the Spitzenkörper core in the hyphal tip as well as numerous smaller puncta. Three-dimensional data acquired and rendered on a ZEISS ELYRA PS.1 at a xyz resolution of ~20 × 20 × 50 nm^3. (Image provided courtesy of Hye-Seon Kim and Seogchan Kang)

(see Fig. 8.6 in Weisshart 2014). In essence, additional resolution is gained by the individual smaller detector elements, effectively acting as very small pinholes. This resolution can be achieved without the signal loss of traditional LSCMs because signal from all elements can be utilized and reassigned from the entire 32-detector array with appropriate algorithms (see Fig B4 in Weisshart 2014). The relatively recent commercial introduction of Airyscan technology precludes reference to the current literature. However, preliminary Airyscan imaging of living *Saccharomyces cerevisiae* reveals clear improvement in S/N and resolution in mCherry and GFP-labeled membranes when compared to a single frame average LSCM (Fig. 8.6). Airyscan has clear advantages including increased scan speeds, little and no averaging and the ability to detect low-level fluorescent signals (i.e., endogenous expression). Unlike super-resolution techniques such as SIM and localization microscopy (Chap. 3), which require imaging in close proximity to the coverslip (i.e., 20 um or less for optimal results), Airyscan data can be collected deep within tissues (agar for fungal cultures). Indeed, this method excels under these light limiting, scattering conditions since the technology is less sensitive to the associated optical aberrations. As such, fixed or living samples traditionally intractable or very challenging for confocal or super-resolution based on weak signals, fast kinetics, or tissue depth (i.e., host–pathogen interactions) can be directly and readily imaged.

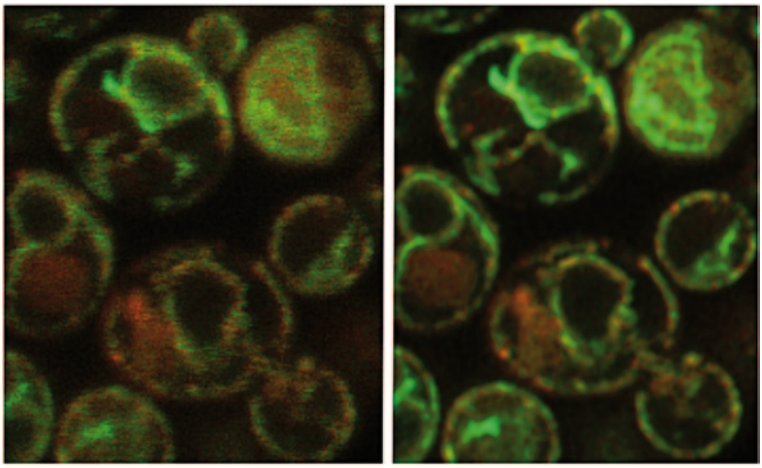

Fig. 8.6 Comparison of LSCM *(left)* and Airyscan imaging *(right)* of living *Saccharomyces cerevisiae* yeast cells. Live yeast cells expressing enhanced green fluorescent protein (eGFP) *(green)* and mCherry *(red)* fusion proteins both targeting the endoplasmic reticulum showed significantly improved resolution and S/N using the Airyscan array detector *(right image)* when compared to a traditional LSCM GaAsP detector *(left image)* when imaged under the same conditions. Data were acquired at the Zeiss Microscopy Labs, without averaging, on a ZEISS LSM880 with Airyscan detector. (Images provided courtesy of Carissa Young and Jeff Caplan)

As previously discussed, localization microscopy is often challenged by long acquisition and processing times that limit its utility for highly dynamic events. When kinetics is critical, other new tools deserve a closer look to help address those types of problems. Bessel beam plane illumination microscopy (Planchon et al. 2011) is one of a family of optical techniques that form a laser excitation sheet within the sample (Reynaud et al. 2015), thus creating an inherent optical section that illuminates an entire optical plane simultaneously rather than scanning a line or array of spots. While not fundamentally a super-resolution technique, this approach offers rapid imaging and improved sensitivity which lends itself to capturing full 3D volumes several orders of magnitude faster than most other optical sectioning methods. Bessel beam plane illumination has specific advantages over other plane illumination techniques as it is able to create much thinner planes and capture nearly 200 planes per second in the *z*-axis in living cells (Planchon et al. 2011). It can be expected that plane-illumination microscopy has the potential to fill a void in high-resolution and high-sensitivity 3D imaging of subcellular dynamics in living samples, including localization-based super-resolution microscopy (Zanacchi et al. 2011). Specifically, the potential to collect multiple, multicolor stacks every second from individual hyphal tips is very attractive for understanding the Spitzenkörper, polarisome, or anastomosis with unprecedented clarity.

Similar to how Bessel beam illumination accelerates 3D acquisition for LM, HS-AFM overcomes the relatively slow raster rate of scanning probe methods, typically requiring 30 s–30 min for high-resolution images (Chap. 7). The development of HS-AFM means that it is now possible to track changes in live cell mechanics

and ultrastructure during dynamic processes. High speed with minimal impact was achieved by minimizing time delays in the feedback loop, dampening mechanical vibrations associated with fast scanning and developing more elaborate feedback control (reviewed in Ando et al. 2013). While performance relates to imaging conditions, HS-AFM can image fragile biological molecules in < 100 ms without structural or functional perturbation, allowing detailed mechanistic visualization in real time. High speed force mapping has been used to monitor cytoskeletal reorganization and growth, cell blebbing, and endocytic pit formation (Braunsmann 2014) and HS-AFM with exceptionally long and nm-sharp AFM tips has resolved filopodia morphogenesis, membrane ruffles, pit formation, and endocytosis in cultured cells at nm-s spatiotemporal resolution (Shibata et al. 2015). Although HS-AFM has yet to be applied to fungal cells, it has resolved the nanostructure of two Gram negative bacteria (Oestreicher 2015) and kinetics of fungal enzymes (Igarashi et al. 2012; Paslay et al. 2013; Shibafuji et al. 2014), demonstrating its applicability. For integrated correlative microscopes, HS-AFM enables simultaneous imaging with speeds more comparable to optical methods.

8.6 Conclusion

This arsenal of cutting-edge technologies is already generating new insights into complex biological systems, ushering in a new era of microscopic exploration. Concomitantly, the latest array of biomarkers, including sensors, FP fusions targeted to specific molecules of interest, and dyes targeting organelles, cell structures, and proteins, can offer unlimited combinations for adaptation to mycological systems. Unprecedented volumetric data from 3D microscopy, including electron, X-ray, and super-resolution, can be used to understand cell structure and function, developmental biology, and tissue architecture for fungal biology. Correlative microscopy, with sophisticated automated software for hybrid and multi-instrument approaches, offers multidimensional and multiscale information from different modes that can span an enormous field of view range (Å—mm). Ultimately, such approaches enable a holistic perspective of fungi at ultrahigh resolutions with novel insights about corresponding chemical, biophysical, and spatial relationships. Finally, the latest developments in optical and scanning probe microscopes vastly improve imaging time, enabling exploration of fungal phenomena in real time. We anticipate that these advances, if harnessed, will have immeasurable impact on our understanding of mycology.

Acknowledgments TESD thanks Spencer Zwarych for collecting the LM and AFM data, and Geremy Lague for photographing Supriya Bhat and the AFM setup shown in Fig. 8.3. Special thanks to Drs. Kathleen Gough, Catherine Liao, Hans Bechtel and Michael Martin and Susan Kaminskyj for the collaborative data collection, analysis and sample preparation for SINS at ALS (Berkeley), and to Dr. Gough for kindly preparing Fig. 8.4.

A very special thanks to Dr. Seogchan Kang and Dr. Hye-Seon Kim for permission to use the 3D super-resolution data, and Dr. Jeff Caplan and Dr. Carissa Young for their efforts and permission to use Airyscan and 3D FESEM/FIB images of yeast.

References

Abbé E (1873) Über einen neuen Beleuchtungsapparat am Mikroskop. Arch mikrosk Anat 9:469–480

Agronskaia AV, Valentijn JA, van Driel LF, Schneijdenberg CT, Humbel BM, van Bergen en Henegouwen PM, Verkleij AJ, Koster AJ, Gerritsen HC (2008) Integrated fluorescence and transmission electron microscopy. J Struct Biol 164:183–189

Akerboom J, Chen T-W, Wardill TJ, Tian L, Marvin JS, Mutlu S, Caldero NC, Esposti F, Borghuis BG, Richard Sun XR, Gordus A, Orger MB, Portugues R, Engert F, Macklin JJ, Filosa A, Aggarwal A, Kerr RA, Takagi R, Kracun S, Shigetomi E, Khakh BS, Baier H, Lagnado L, Wang SS-H, Bargmann CI, Kimmel BE, Jayaraman V, Svoboda K, Kim DS, Schreiter ER, Looger LL (2012) Optimization of a GCaMP calcium indicator for neural activity imaging. J Neurosci 32:13819–13840

Ando T, Uchihashi T, Kodera N (2013) High-speed AFM and applications to biomolecular systems. Annu Rev Biophys 42:393–414

Andrews JS, Rolfe SA, Huang WE, Scholes JD, Banwart SA (2010) Biofilm formation in environmental bacteria is influenced by different macromolecules depending on genus and species. Environ Microbiol 12:2496–2507

Bacia K, Schwille P (2003) A dynamic view of cellular processes by in vivo fluorescence auto- and cross-correlation spectroscopy. Methods 29:74–85

Baddeley D, Cannell MB, Soeller C (2011) Three-dimensional sub-100 nm super-resolution imaging of biological samples using a phase ramp in the objective pupil. Nano Res 4:589–598

Bechtel HA, Muller EA, Olmon RL, Martin MC, Raschke MB (2014) Ultrabroadband infrared nanospectroscopic imaging. Proc Natl Acad Sci U S A 111:7191–7196

Belousov VV, Fradkov AF, Lukyanov KA, Staroverov DB, Shakhbazov KS, Terskikh AV, Lukyanov S (2006) Genetically encoded fluorescent indicator for intracellular hydrogen peroxide. Nat Methods 3:281–286

Berweger S, Nguyen DM, Muller EA, Bechtel HA, Perkins TT, Raschke MB (2013) Nano-chemical infrared imaging of membrane proteins in lipid bilayers. J Am Chem Soc 135:18292–18295

Bhat B, Vantomme A, Yost D et al (2015a) Oxidative stress and metabolic perturbations in *Escherichia coli* exposed to sublethal levels of 2,4-dichlorophenoxyacetic acid. Chemosphere 135:453–461

Bhat B, McGrath D et al (2015b) *Rhizobium leguminosarum* bv. *viciae* 3841 adapts to 2,4-dichlorophenoxyacetic acid with "auxin-like" morphological changes, cell envelope remodeling and upregulation of central metabolic pathways. PLoS ONE 10:e0123813

Bourett TM, Czymmek KJ, Howard RJ (1998) An improved method for affinity probe localization in whole cells of filamentous fungi. Fungal Genet Biol 24:3–13

Braunsmann C, Seifert J, Rheinlaender J, Schäffer TE (2014) High-speed force mapping on living cells with a small cantilever atomic force microscope. Rev Sci Instrum 85:073703

Caplan J, Niethammer M, Taylor II RM II, Czymmek KJ (2011) The power of correlative microscopy: multi-modal, multi-scale, multi-dimensional. Curr Opin Struct Biol 21:686–693

Chacko JV, Canale C, Harke B, Diaspro A (2013a) Sub-diffraction nano manipulation using STED AFM. PLoS ONE 8:e66608

Chacko JV, Zanacchi FC, Diaspro A (2013b) Probing cytoskeletal structures by coupling optical superresolution and AFM techniques for a correlative approach. Cytoskeleton 70:729–740

Chacko JV, Harke B, Canale C, Diaspro A (2014) Cellular level nanomanipulation using atomic force microscope aided with superresolution imaging. J Biomed Opt 19:105003

Chakravarty R, Goel S, Cai W (2014) Nanobody: the "Magic Bullet" for molecular imaging? Theranostics 4:386–398

Chang WT, Yang YC, Lu HH, Li IL, Liau I (2010) Spatiotemporal characterization of phagocytic NADPH oxidase and oxidative destruction of intraphagosomal organisms in vivo using autofluorescence imaging and Raman microspectroscopy. J Am Chem Soc 132:1744–1745

Czymmek KJ, Bourett TM, Dezwaan TM, Sweigard JA, Howard RJ (2002) Utility of cytoplasmic fluorescent proteins for live-cell imaging of *Magnaporthe grisea* in planta. Mycologia 94:280–289

Czymmek KJ, Bourett TM, Howard RJ (2004) Fluorescent protein probes in fungi. In: Savidge T, Charalabos P (Imaging Meds) Methods in microbiology (microbial imaging), vol 34. Academic Press, New York, pp 27–32

Czymmek KJ, Bourett TM, Shao Y, Dezwaan TM, Sweigard JA, Howard RJ (2005) Live-cell imaging of tubulin in the filamentous fungus *Magnaporthe grisea* treated with anti-microtubule and anti-microfilament agents. Protoplasma 225:23–32

Denk W, Horstmann H (2004) Serial block-face scanning electron microscopy to reconstruct three-dimensional tissue nanostructure. PLoS Biol 2:e329

den Hoedt SV, Effting APJ, Haring MT (2014) The SECOM platform: an integrated CLEM solution. Microsc Microanal 20(Supp 3):1006–1007

Efimov AE, Tonevitsky AG, Dittrich M, Matsko NB (2007) Atomic force microscope (AFM) combined with the ultramicrotome: a novel device for the serial section tomography and AFM/TEM complementary structural analysis of biological and polymer samples. J Microsc 226:207–217

Faas FG, Bárcena M, Agronskaia AV, Gerritsen HC, Moscicka KB, Diebolder CA, van Driel LF, Limpens RW, Bos E, Ravelli RB, Koning RI, Koster AJ (2013) Localization of fluorescently labeled structures in frozen-hydrated samples using integrated light electron microscopy. J Struct Biol 181:283–290

Frommer WB, Davidson MW, Campbell RE (2009) Genetically encoded biosensors based on engineered fluorescent proteins. Chem Soc Rev 38:2833–2841

Gamble RC, West PG (1994) Scanning force microscope with integrated optics and cantilever mount. US Patent # 5291775 A, March 8

Handschuh S, Baeumler N, Schwaha T, Ruthensteiner B (2013) A correlative approach for combining microCT, light and transmission electron microscopy in a single 3D scenario. Front Zool 10:44. doi:10.1186/1742-9994-10-44

Harke B, Chacko JV, Haschke H, Canale C, Diaspro A (2012) A novel nanoscopic tool by combining AFM with STED microscopy. Opt Nanoscopy 1:3

Harris SD, Read ND, Roberson RW, Shaw B, Seiler S, Plamann M, Momany M (2005) Spitzenkörper meets polarisome: microscopy, genetics, and genomics converge. Eukaryot Cell 4:225–229

Hayworth KJ, Morgan JL, Schalek R, Berger DR, Hildebrand DGC, Lichtman JW (2014) Imaging ATUM ultrathin section libraries with WaferMapper: a multi-scale approach to EM reconstruction of neural circuits. Front Neural Circuits 8:1–18

Helmstaedter M, Briggman KL, Denk W (2008) 3D structural imaging of the brain with photons and electrons. Curr Opin Neurobiol 18:633–407

Hickey PC, Swift SR, Roca MG, Read ND (2004) Live-cell imaging of filamentous fungi using vital fluorescent dyes and confocal microscopy. In: Savidge T, Charalabos P (eds) Methods in microbiology (microbial imaging), vol 34. Academic Press, New York, pp 63–87

Hillenbrand R, Knoll B, Keilmann F (2001) Pure optical contrast in scattering-type scanning near-field microscopy. J Microsc 202:77–83

Hohmann-Marriott MF, Uchida M, van de Meene AML, Garret M, Hjelm BE, Kokoori S, Roberson RW (2006) Application of electron tomography to fungal ultrastructure studies. New Phytol 172:208–220

Honda A, Adams SR, Sawyer CL, Lev-Ram V, Tsien RY Dostmann WRG (2001) Spatiotemporal dynamics of guanosine 3′,5′-cyclic monophosphate revealed by genetically encoded, fluorescent indicator. Proc Natl Acad Sci U S A 98:2437–2442

Howard RJ, Aist JR (1979) Hyphal tip cell ultrastructure of the fungus Fusarium:improved preservation by freeze-substitution. J Ultrastruct Res. 66:224–234

Hughes L, Hawes C, Monteith S, Vaughan S (2014) Serial block face scanning electron microscopy—the future of cell ultrastructure imaging. Protoplasma 251:395–401

Igarashi K, Uchihashi T, Koivula A, Wada M, Kimura S, Penttilä M, Ando T, Samejima M (2012) Visualization of cellobiohydrolase I from *Trichoderma reesei* moving on crystalline cellulose using high-speed atomic force microscopy. Methods Enzymol 510:169–182

Imamura H, Nhat KP, Togawa H, Saito K, Iino R, Kato-Yamada Y, Nagai T, Noji H (2009) Visualization of ATP levels inside single living cells with fluorescence resonance energy transfer-based genetically encoded indicators. Proc Natl Acad Sci U S A 106:15651–15656

Jun AD, Signo K, Yost CM, Dahms TES (2011) Atomic force microscopy of a ctpA mutant in *Rhizobium leguminosarum* reveals surface property defects linking ctpA function to biofilm formation. Microbiol 157:3049–3058

Jungmann R, Avendaño MS, Woehrstein JB, Dai M, Shih WM, Yin P (2014) Multiplexed 3D cellular super-resolution imaging with DNA-PAINT and Exchange-PAINT. Nat Methods 11:313–318

Kaminskyj SGW, Dahms TES (2008) High spatial resolution surface imaging and analysis of fungal cells using SEM and AFM. Micron 39:349–361

Kanemaru T, Hirata K, Takasu S, Isobe S, Mizuki K, Mataka S, Nakamura K (2009) A fluorescence scanning electron microscope Ultramicroscopy 109:344–349

Kankanala P, Czymmek K, Valent B (2007) Roles for rice membrane dynamics and plasmodesmata during biotrophic invasion by the blast fungus. Plant Cell 19:706–724

Kim H-S, Czymmek KJ, Patel A, Modla S, Nohe A, Duncan R, Gilroy S, Kang S (2012) Expression of the Cameleon calcium biosensor in fungi reveals distinct Ca^{2+} signatures associated with polarized growth, development, and pathogenesis. Fungal Genet Biol 49:589–601

Lal R, Arnsdorf MF (2010) Multidimensional atomic force microscopy for drug discovery: a versatile tool for defining targets, designing therapeutics and monitoring their efficacy. Life Sci 86:545–562

Lausch V, Hermann P, Laue M, Bannert N (2014) Silicon nitride grids are compatible with correlative negative staining electron microscopy and tip-enhanced Raman spectroscopy for use in the detection of micro-organisms. J Appl Microbiol 116:1521–1530

Le NC, Yokokawa R, Dao DV, Nguyen TD, Wells JC, Sugiyama S (2009) Versatile microfluidic total internal reflection (TIR)-based devices: application to microbeads velocity measurement and single molecule detection with upright and inverted microscope. Lab Chip 9:244–250

Li H, Wang H, Huang D, Liang L, Gu Y, Liang C, Xu S, Xu W (2014) Note: Raman microspectroscopy integrated with fluorescence and dark field imaging. Rev Sci Instrum 85:056109

Löschberger A, Franke C, Krohne G, van de Linde S, Sauer M (2014) Correlative super-resolution fluorescence and electron microscopy of the nuclear pore complex with molecular resolution. J Cell Sci 127:4351–4355

Luo KQ, Yu VC, Pu Y, Chang DC (2001) Application of the fluorescence resonance energy transfer method for studying the dynamics of caspase-3 activation during UV-induced apoptosis in living HeLa cells. Biochem Biophys Res Commun 283:1054–1060

Ma H, Snook L, Kaminskyj S, Dahms TES (2005) Surface ultrastructure and elasticity in growing tips and mature regions of *Aspergillus* hyphae describe wall maturation. Microbiol 151:3679–3688

Ma H, Snook L, Tian C, Kaminskyj S, Dahms TES (2006) Fungal surface remodeling visualized by atomic force microscopy. Mycol Res 110:879–886

Martell JD, Deerinck TJ, Sancak Y, Poulos TL, Mootha VK, Sosinsky GE, Ellisman MH, Ting AY (2012) Engineered ascorbate peroxidase as a genetically encoded reporter for electron microscopy. Nat Biotechnol 30:1143–1148

Micheva KD, Smith SJ (2007) Array tomography: a new tool for imaging the molecular architecture and ultrastructure of neural circuits. Neuron 55:25–36

Miesenböck G, De Angelis DA, Rothman JE (1998) Visualizing secretion and synaptic transmission with pH-sensitive green fluorescent proteins. Nature 394:192–195

Miyawaki A, Llopis J, Heim R, McCaffery JM, Adams JA, Ikura M, Tsien RY (1997) Fluorescent indicators for Ca^{2+} based on green fluorescent proteins and calmodulin. Nature 388:882–887

Modla S, Caplan JL, Czymmek KJ, Lee JY (2015) Localization of fluorescently tagged protein to plasmodesmata by correlative light and electron microscopy. Methods Mol Biol 1217:121–133

Monserrate A, Casado S, Flors C (2014) Correlative atomic force microscopy and localization-based super-resolution microscopy: revealing labelling and image reconstruction artefacts. Chem Phys Chem 15:647–650

Nagai T, Yamada S, Tominaga T, Ichikawa M, Miyawaki A (2004) Expanded dynamic range of fluorescent indicators for Ca_{2+} by circularly permuted yellow fluorescent proteins. Proc Natl Acad Sci, U S A 101:10554–10559

Nagao E, Dvorak JA (1998) An integrated approach to the study of living cells by atomic force microscopy. J Microsc 191:8–19

Narayan K, Danielson CM, Lagarec K, Lowekamp BC, Coffman P, Laquerre A, Phaneuf MW, Hope TJ, Subramaniam S (2014) Multi-resolution correlative focused ion beam scanning electron microscopy: applications to cell biology. J Struct Biol 185:278–284

Nelson: http://onlinelibrary.wiley.com/doi/10.1111/j.1365-2958.2004.04066.x/abstract: Nelson G, Kozlova-Zwinderman O, Collis AJ, Knight MR, Fincham JRS, Stanger CP, Renwick A, Hessing JGM, Punt PJ, Van Den Hondel CAMJJ, Read, ND (2004) Calcium measurement in living filamentous fungi expressing codon-optimized aequorin. Mol Microbiol 52:1437–1450

Newman RH, Fosbrink MD, Zhang J (2011) Genetically encodable fluorescent biosensors for tracking signaling dynamics in living cells. Chem Rev 111:3614–3666

Oestreicher Z, Taoka A, Fukumori Y (2015) A comparison of the surface nanostructure from two different types of gram-negative cells: *Escherichia coli* and *Rhodobacter sphaeroides*. Micron 72C:8–14

Okumoto S, Jones A, Frommer WB (2012) Quantitative imaging with fluorescent biosensors. Annu Rev Plant Biol 63:663–706

Paslay LC, Falgout L, Savin DA, Heinhorst S, Cannon GC, Morgan SE (2013) Kinetics and control of self-assembly of ABH1 hydrophobin from the edible white button mushroom. Biomacromolecules 14:2283–2293

Paul BC, El-Ganiny AM, Abbas M, Kaminskyj SGW, Dahms TES (2011) Quantifying the importance of galacto-furanose in *Aspergillus nidulans* hyphal wall surface organization by atomic force microscopy. Eukaryot Cell 10:646–653

Paul BC, Snook L, Ma H, Dahms TES (2013) High-resolution imaging and force spectroscopy of fungal hyphal cells by atomic force microscopy. In: Gupta VK, Tuohy MG, Ayyachamy M, Turner KM, O'Donovan A (eds) Laboratory protocols in fungal biology. Springer, USA

Perkel JM (2014) Correlating Light and Electron Microscopy. BioTechniques 57:172–177

Pertz O, Hodgson L, Klemke RL, Hahn KM (2006) Spatiotemporal dynamics of RhoA activity in migrating cells. Nature 440:1069–1072

Planchon TA, Gao L, Milkie DE, Davidson MW, Galbraith JA, Galbrait CG, Betzig E (2011) Rapid three-dimensional isotropic imaging of living cells using Bessel beam plane illumination. Nat Methods 8:417–423

Reuben S, Banas K, Banas A, Swarup S (2014) Combination of synchrotron radiation-based Fourier transforms infrared microspectroscopy and confocal laser scanning microscopy to understand spatial heterogeneity in aquatic multispecies biofilms. Water Res 64:123–133

Reynaud EG, Peychl J, Huisken J, Tomancak P (2015) Guide to light-sheet microscopy for adventurous biologists. Nat Methods 12:30–34

Ries J, Kaplan C, Platonova E, Eghlidi H, Ewers H (2012) A simple, versatile method for GFP-based super-resolution microscopy via nanobodies. Nat Methods 9:582–4

Riquelme M, Roberson RW, McDaniel DP Bartnicki-Garcıa S (2002) The effects of ropy-1 mutation on cytoplasmic organization and intracellular motility in mature hyphae of *Neurospora crassa*. Fungal Genet Biol 37:171–179

Sandercock JR (1987) A dynamic antivibration system. Proc SPIE 0732, 1st Intl Conf on Vibration Control in Optics and Metrology, 157. doi:10.1117/12.937916

Sato M, Hida N, Ozawa T, Umezawa Y (2000) Fluorescent indicators for cyclic GMP based on cyclic GMP-dependent protein kinase Ialpha and green fluorescent proteins. Anal Chem 72:5918–5924

Schleifenbaum A, Stier G, Gasch A, Sattler M, Schultz C (2004) Genetically encoded FRET probe for PKC activity based on pleckstrin. J Am Chem Soc 126:11786–11787

Schulz O, Zhao Z, Ward A, Koenig M, Koberling F, Liu Y, Enderlein J, Yan H, Ros R (2013) Tip induced fluorescence quenching for nanometer optical and topographical resolution. Opt Nanoscopy 2:1

Shibafuji Y, Nakamura A, Uchihashi T, Sugimoto N, Fukuda S, Watanabe H, Samejima M, Ando T, Noji H, Koivula A, Igarashi K, Iino R (2014) Single-molecule imaging analysis of elementary reaction steps of *Trichoderma reesei* cellobiohydrolase I (Cel7A) hydrolyzing crystalline cellulose Iα and IIII. J Biol Chem 289:14056–14065

Shibata M, Uchihashi T, Ando T, Yasuda R (2015) Long-tip high-speed atomic force microscopy for nanometer-scale imaging in live cells. Sci Rep 5:8724

Shu X, Lev-Ram V, Deerinck TK, Qi Y, Ramko EB, Davidson MW, Jin Y, Ellisman MH, Tsergevelakis GJ, Soliman D, Omar M, Ntziachristos V (2014) Hybrid multiphoton and optoacoustic microscope. Opt Lett 39:1819–1822

Smith C (2012) Two microscopes are better than one. Nature 492:293–297

Stemmer A (1995) A hybrid scanning force and light microscope for surface imaging and three-dimensional optical sectioning in differential interference contrast. J Microsc 178:28–36

Subach FV, Subach OM, Gundorov IS, Morozova KS, Piatkevich KD, Cuervo AM, Verkhusha VV (2009) Monomeric fluorescent timers that change color from blue to red report on cellular trafficking. Nat Chem Biol 5:118–126

Terskikh A, Fradkov A, Ermakova G, Zaraisky A, Tan P, Kajava AV, Zhao X, Lukyanov S, Matz M, Kim S, Weissman I, Siebert P (2000) "Fluorescent Timer": protein that changes color with time. Science 290:1585–1588

Tsien RY (2011) A genetically encoded tag for correlated light and electron microscopy of intact cells, tissues, and organisms. PLoS Biol 9:e1001041

Tsutsui H, Karasawa S, Okamura Y, Miyawaki A (2008) Improving membrane voltage measurements using FRET with new fluorescent proteins. Nat Methods 7:683–685

van Manen HJ, Otto C (2007) Hybrid confocal Raman fluorescence microscopy on single cells using semiconductor quantum dots. Nano Lett 7:1631–1636

Varnai P, Balla T (2007) Visualization and manipulation of phosphoinsitide dynamics in live cells using engineered protein dynamics. Eur J Physiol 455:69–82

Wei D, Jacobs S, Modla S, Zhang S, Young CL, Cirino R, Caplan J, Czymmek K (2012) High-resolution three-dimensional reconstruction of a whole yeast cell using focused-ion beam scanning electron microscopy. Biotechniques 53(1):41–48

Weisshart K (2014) The basic principle of airyscanning, pp 1–11. ZEISS

Williams PA, Papadakis SJ, Flavo MR, Patel AM, Sinclair M, Seeger A, Hesler A, Taylor RM, Washburn S, Superfine R (2002) Controlled placement of an individual carbon nanotube onto a microelectromechanical structure. Appl Phys Lett 80:2574–2576

Wu J, Zheng G, Lee LM (2012) Optical imaging techniques in microfluidics and their applications. Lab Chip 12:3566–3575

Xu X, Gerard ALV, Huang BCB, Anderson DC, Payan DG, Luo Y (1998) Detection of programmed cell death using fluorescence energy transfer. Nucleic Acids Res 26:2034–2035

Young CL, Raden DL, Caplan J, Czymmek K, Robinson AS (2012) Optimized cassettes for live-cell imaging of proteins and high-resolution in yeast. Yeast 29:119–136

Zaccolo M, De Giorgi F, Cho CY, Feng L, Knapp T, Negulescu PA, Taylor SS, Tsien RY Pozzan T (2000) A genetically encoded, fluorescent indicator for cyclic AMP in living cells. Nat Cell Biol 2:25–29

Zanacchi FC, Lavagnino Z, Donnorso MP, Bue AD, Furia L, Faretta M, Diaspro A (2011) Live-cell 3D super-resolution imaging in thick biological samples. Nat Methods 8:1047–1049

Zhang C, Czymmek KJ, Shapiro AD (2003) Nitric oxide does not trigger early programmed cell death events but may contribute to cell-to-cell signaling governing progression of the *Arabidopsis* hypersensitive response. Mol Plant Microbe Interact 16:962–972

Zhao W, Tian Y, Cai M, Wang F, Wu J, Gao J, Liu S, Jiang J, Jiang S, Wang H (2014) Studying the nucleated mammalian cell membrane by single molecule approaches. PLoS ONE 9:e91595